Spin density wave order and fluctuations in Mn_3Si : A transport study

Frank Steckel,[1,2,*] Steven Rodan,[1] Regina Hermann,[1] Christian G. F. Blum,[1] Sabine Wurmehl,[1,2] Bernd Büchner,[1,2,3] and Christian Hess[1,3,†]

[1]*Leibniz-Institute for Solid State and Materials Research, IFW-Dresden, 01171 Dresden, Germany*

[2]*Institut für Festkörperphysik, TU Dresden, 01069 Dresden, Germany*

[3]*Center for Transport and Devices, Technische Universität Dresden, 01069 Dresden, Germany*

(Received 6 September 2013; revised manuscript received 24 September 2014; published 14 October 2014)

We present a comprehensive transport investigation of the itinerant antiferromagnet Mn_3Si which undergoes a spin density wave (SDW) order below $T_N \sim 21.3$ K. The electrical resistivity, the thermal conductivity, and the Hall, Seebeck, and Nernst effects exhibit pronounced anomalies at the SDW transition. At temperatures higher than T_N our data provide strong evidence for a large fluctuation regime which extends up to ∼200 K in the resistivity, the Seebeck effect, and the Nernst effect. From the comparison of our results with other prototype SDW materials, viz., LaFeAsO and chromium, we conclude that many of the observed features are of generic character.

DOI: 10.1103/PhysRevB.90.134411 PACS number(s): 72.15.−v, 42.50.Lc, 75.30.Mb, 75.30.Fv

I. INTRODUCTION

Intrinsic electronic ordering phenomena have in recent years been a focus of condensed matter research in the context of unconventional quantum phenomena, e.g., unconventional superconductivity. For example, in the cuprate high-temperature superconductors it is well established that electronic ordering states, which give rise to inhomogeneous charge and spin distributions, exist and seemingly compete with the superconducting state [1–7]. Another important material class is that of the more recently discovered iron-pnictide superconductors [8]. Here, superconductivity emerges upon the suppression of a spin density wave (SDW) state, which suggests that the magnetic and superconducting ground states compete for the electrons near the Fermi level [9–15], and thus, further underpins the importance of electronic order for rationalizing unconventional superconductivity. Electronic ordering states such as SDW or charge density waves are intimately connected with reconstructions of the Fermi surface topology with respect to the nonordered states, which cause anomalous behavior of many physical properties at the phase transition. The transport properties are of fundamental importance as the electrons at the Fermi level are directly probed. This concerns, in addition to the well-known quantities of resistivity, the Hall effect, and the Seebeck effect, also the Nernst effect, which came into focus recently because of its sensitivity to subtle Fermi-surface changes and fluctuations [16–23]. For example, in superconductors an enhanced Nernst coefficient occurs above the critical temperature due to short-lived Cooper pairs [24]. Similar observations for cuprate superconductors have led to interpreting the pseudogap phase within such a scenario [25,26]. On the other hand, an enhanced Nernst effect has also received strong attention as a sensitive probe for Fermi-surface reconstructions due to electronic order [16,17,19,20].

In this paper we take the impact of SDW ordering on the transport coefficients under scrutiny by investigating the transport properties of the itinerant antiferromagnet Mn_3Si which undergoes a SDW transition at about 25 K [27–31]. We study in particular the electrical resistivity, thermal conductivity, Hall effect, Seebeck effect, and Nernst effect in the temperature range from 10 K up to 300 K. Clear anomalies are observed at the SDW transition which confirm it to be at ∼21 K and give strong evidence for a large fluctuation regime which extends up to ∼200 K in the resistivity, as well as in the Seebeck and Nernst effects. We compare our results with other prototype SDW materials, viz., the iron arsenide LaFeAsO and the classical SDW prototype chromium.

Mn_3Si is an intermetallic compound with a lattice constant of $a = 5.722$ Å [32]. It belongs to the broad family of $L2_1$ Heusler compounds. In the typical Heusler notation the compound is written as $Mn^{II}_2Mn^{I}Si$ with two different crystallographic manganese sites. The structure is described by four fcc-lattices with the following positions: Mn^{I} at (0,0,0), Mn^{II} at $(\frac{1}{4},\frac{1}{4},\frac{1}{4})$ and $(\frac{3}{4},\frac{3}{4},\frac{3}{4})$, and Si at $(\frac{1}{2},\frac{1}{2},\frac{1}{2})$ in units of the lattice constant a. Through the different surroundings of the Mn atoms, they have different magnetic moments $\mu_{Mn^{I}} = 1.72\mu_B$ and $\mu_{Mn^{II}} = 0.19\mu_B$ found by neutron diffraction [27]. Additional to the asymmetry of the magnetic moments, neutron diffraction experiments revealed an incommensurable SDW with the wave vector $\vec{q} = 4.25(2\pi/a) \times (1,1,1)$ [33]. Thus Mn_3Si is an itinerant antiferromagnet with an incommensurate spin spiral structure [27–30]. Recent synchrotron x-ray diffraction data provide evidence of a CDW accompanying the SDW at low temperatures [34]. Aside from these experimental results, theoretical work suggests the weak magnetic moment of Mn^{II} to be induced by the Mn^{I} moment [35], consistent with the Kübler rule [36,37]. Further theoretical work predicted two nesting vectors of which one corresponds to the one that is experimentally found [38,39]. Early publications concerning Mn_3Si suggested it to be a possible candidate for half-metallic antiferromagnetism [31,40–43], which would represent a new paradigm of itinerant magnetism. However, experimental evidence for such a ground state remains elusive.

II. EXPERIMENTAL

The Mn_3Si single crystalline sample was grown [44] by using a two-phase radio frequency floating-zone method, described in detail elsewhere [45]. The orientation of the

*f.steckel@ifw-dresden.de

†c.hess@ifw-dresden.de

crystals was determined by using the x-ray Laue backscattering method. Our sample has negligible magnetic impurities (less than 0.08 vol%) which cause a slight remanent magnetic moment, which is unchanged by temperature variation [44]. The specific-heat measurements were performed with a Physical Property Measurement System (PPMS, Quantum Design). All measurements shown here were performed on the same Mn_3Si sample with a cuboid shape of the size $0.5 \times 0.5 \times 2.25$ mm^3. Electric and thermal currents were forced along the long axis of the crystal which was cut to be the [110] axis. Except for the specific heat all data were taken with a homemade device. The resistivity and Hall measurements were performed as a function of temperature by using a standard four-probe technique. During the Hall effect measurements the transverse resistivity ρ_{xy} was linear up to 15 T. The Hall coefficient data were calculated by antisymmetrizing ρ_{xy} in magnetic field and taking the slope of the linear curve in $|\mu_0 H|$. All electrically conducting contacts were made by using a silver epoxy glue. For the heat conductivity, the Seebeck effect, and the Nernst effect measurements we used a chip resistor as heater in a steady-state method and a Au-chromel differential thermocouple to measure the temperature gradient ∇T along the sample [46]. We measured the Seebeck effect (also called thermopower) at the same time as the heat conductivity by attaching two electrical contacts to the sample along the temperature gradient. The Nernst effect was measured in magnetic fields up to 14 T, with the electrical contacts perpendicular to the thermal gradient. The magnetic field was applied perpendicular to these two directions, and the Nernst signal was linear in field. The Nernst coefficient was calculated by measuring the Nernst signal at every shown temperature at 14 T and then antisymmetrizing the data with two different magnetic-field directions.

III. RESULTS AND DISCUSSION

A. Heat capacity

The heat capacity is shown in Fig. 1(a). Except for the pronounced anomaly with a maximum at $T = 21.3$ K, the heat capacity is monotonically rising with increasing temperature. It resembles the behavior seen in earlier measurements on polycrystals [31]. In order to determine the magnetic ordering temperature we refrain from applying the entropy-conserving construction. Instead of a smeared out and rather broad peak structure which one would expect for a canonical second-order type transition, the anomaly possesses a characteristic λ shape, which points towards strong fluctuations [see inset of Fig. 1(a)]. In this case we find the transition temperature from the paramagnetic to the SDW region to be exactly at the peak temperature of the anomaly and thus $T_N \simeq 21.3$ K, which agrees rather well with previous reports [27,31]. The entropy-conserving construction would yield a somewhat higher T_N around ∼24 K. At the lowest accessible temperatures we observe $C \sim \gamma T + \beta T^3$ with $\gamma = 62.5$ mJ mol^{-1} K^{-2} and $\beta = 1.28 \times 10^{-3}$ J mol^{-1} K^{-4} deviating less than 10% from the polycrystalline samples [31].

B. Resistivity

In Fig. 1(b) the resistivity is plotted as a function of temperature. The absolute value at room temperature is

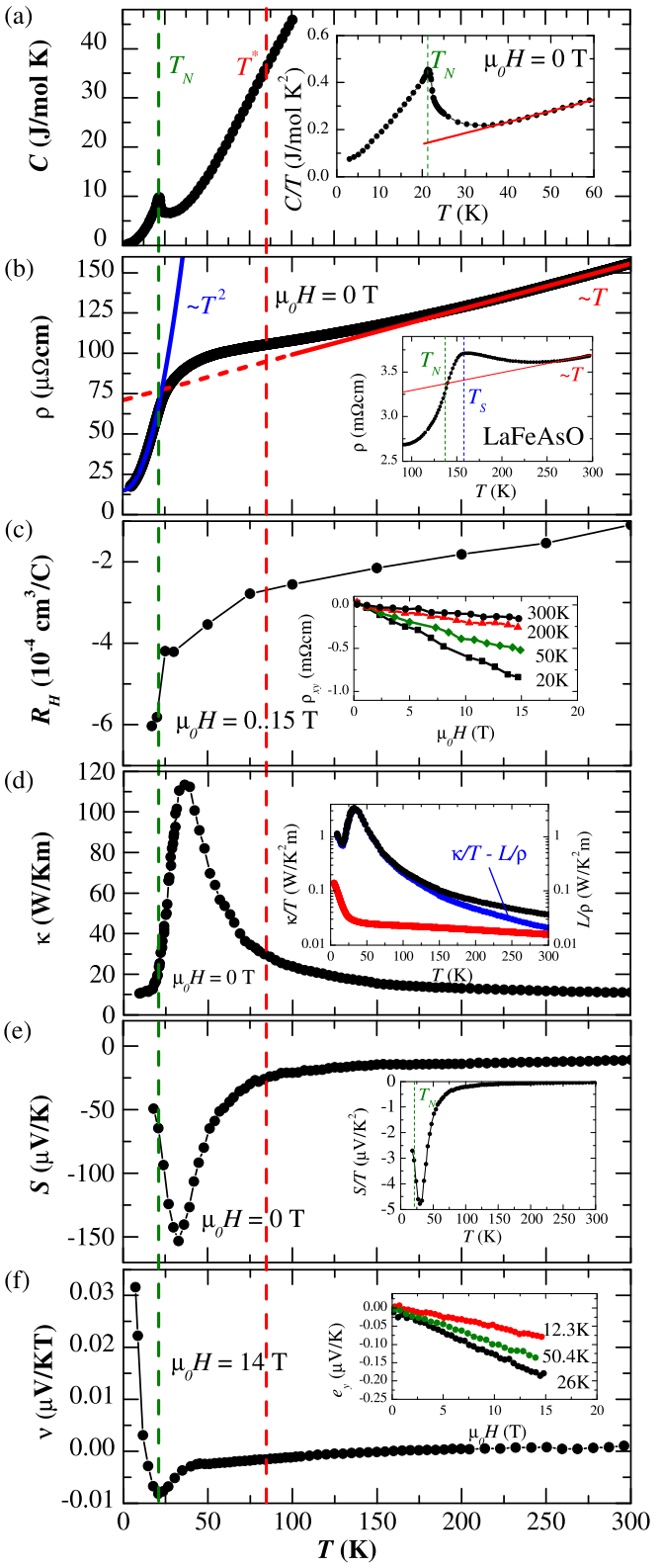

FIG. 1. (Color online) (a) Specific heat, (b) resistivity, (d) thermal conductivity, (c) Hall, (e) Seebeck, and (f) Nernst coefficient of Mn_3Si. Inset (a): construction of T_N. Inset (b): resistivity of LaFeAsO from Hess *et al.* [47]. Inset (c): transverse resistivity ρ_{xy} vs magnetic field. Inset (d): κ/T, L/ρ, and $\kappa/T - L/\rho$ on a log scale. Inset (e): S/T. Inset (f): Nernst signal e_y vs magnetic field.

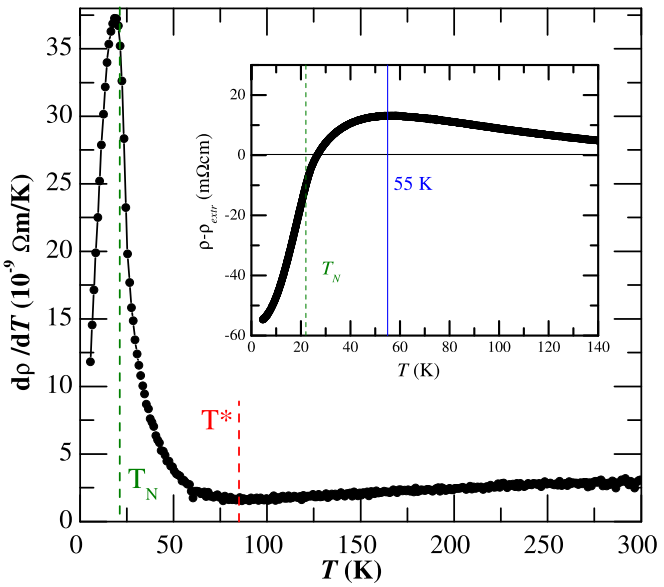

FIG. 2. (Color online) Derivation of the resistivity of Mn_3Si(dots). Inset: resistivity deviation from the extrapolated high-temperature behavior $\rho - \rho_{\mathrm{extr}}$ (dots) solid line marks the temperature 55 K with maximum deviation.

$\rho(300\ \mathrm{K}) = 160\ \mu\Omega$ cm and the extrapolated residual resistance is $\rho_0 = 14.88\ \mu\Omega$ cm, giving a residual resistance ratio (RRR) of ∼10.7 similar to the studied polycrystals [31]. Our measurement resembles previous results on polycrystalline Mn_3Si [31]. At temperatures higher than ∼200 K the resistivity approaches a linearly rising behavior with temperature, a typical characteristic of electron-phonon scattering [expressed in the high-temperature limit of the Grüneisen–Bloch formula [48] as is indicated by the solid line in Fig. 1(b)]. Apparently the resistivity deviates from this linear behavior towards higher values in a temperature region between 25 and 200 K. Below an inflection point at $T^* \approx 85$ K the deviation becomes weaker and reaches a maximum at around 55 K (cf. Fig. 2). At $T < 55$ K, the resistivity starts to decrease stronger and then crosses the extrapolated high-temperature linear T dependence close to T_N. At temperatures below T_N the resistivity decreases further, exhibits an inflection point at $T \sim 20$ K, i.e., nearly exactly at T_N, and shows a crossover to a T^2 dependence which is complete at $T \lesssim 14$ K [indicated by the solid line in Fig. 1(b)].

The deviation of the resistivity from the expected linear high-temperature behavior can only arise if the number of charge carriers or their relaxation rate increases. In fact, inelastic neutron scattering data reveal antiferromagnetic fluctuations preceding the magnetic transition with an unusual large correlation length (∼18 Å) up to high temperatures of ∼200 K [28,33]. We therefore attribute the resistivity enhancement to stem from such fluctuations. In such a scenario, it is natural to expect that both the inverse carrier density and the relaxation rate increase. The change at T^* signals that one of these quantities start to decrease. Since the inverse carrier density is unlikely to increase upon approaching the SDW state, we attribute the changes at T^* to the onset of a decrease of the scattering rate. A plausible explanation is that at some temperature above T_N the correlation length of magnetically ordered areas match with the mean-free path of the electrons. In such patches of incipient SDW order one expects the phase space of carrier scattering to be strongly reduced due to the opening of the SDW gap. At T_N, the magnetic order and the connected Fermi surface reconstruction becomes eventually long range. The strong reduction of the resistivity below T_N therefore is naturally explained by a further reduction of the scattering rate which overcompensates the depletion of carriers in the SDW state. Note that the SDW gap opening seems to be completed at the inflection point at ∼20 K, where the decrease of the resistivity becomes weaker (cf. Fig. 2). This marks the completion of the transition at T_N.

The T^2 dependence of the resistivity at the lowest temperature may be explained with Fermi liquid behavior in the context of strong electron-electron correlation. The quadratic low-temperature behavior of the resistivity with $A = 115.6\ \mathrm{n\Omega\ cm/K^2}$ [cf. Fig. 1(b)] yields the Kadowaki–Woods ratio $A/\gamma^2 = 29.6$ which fits well to previous polycrystalline data [31]. However, another possible explanation is electron scattering off antiferromagnetic spin waves (magnons) in the antiferromagnetic phase [49–51]. However, it seems elusive to discriminate which scenario is dominant from the present data.

It is interesting to compare these findings with resistivity data of other prototype SDW materials. The material LaFeAsO may be viewed as a representative case of the iron arsenide parent compounds exhibiting SDW order. Its magnetic transition occurs at $T_N = 137$ K which is preceded by a structural transition from tetragonal to orthorhombic at $T_S = 160$ K [cf. inset of Fig. 1(b)] [47,52]. The temperature dependence of the resistivity of this compound [47] is remarkably similar to that of Mn_3Si. This concerns almost all the qualitative observations except a low-temperature upturn which is present in the resistivity of LaFeAsO, i.e., the linear high-temperature behavior, the enhanced scattering above T_N, and the strong reduction below, including the inflection point.

The SDW order in Mn_3Si has often been compared with the elementary SDW material Cr [27,31]. Surprisingly, the temperature behavior of the resistivity of Cr is very different because it exhibits a small hump below T_N [53,54].

C. Hall effect

The temperature dependence of the Hall coefficient R_H is shown in Fig. 1(c). R_H is negative over the complete temperature range, which in a one-band model corresponds to electrons as charge carriers. Note that the one-band picture is a simplified approach because Mn_3Si is known to be a multiband metal from band-structure calculations [55].

At 300 K the Hall coefficient is $R_H = -1 \times 10^{-4}\ \mathrm{cm^{-3}/C}$ and increases almost linearly to more negative values upon decreasing the temperature down to T^* where $R_H \approx -2.8 \times 10^{-4}\ \mathrm{cm^{-3}/C}$. Such a weak temperature dependence of R_H is characteristic for multiband materials, e.g., resulting from a thermal redistribution of carriers from occupied states to unoccupied states. Below T^* and again below T_N, $R_H(T)$ changes to more negative values ($R_H \approx -6 \times 10^{-4}\ \mathrm{cm^{-3}/C}$ at 17 K).

The drop of R_H below T_N can clearly be attributed to the SDW order. The qualitative origin of this drop can straightforwardly be connected with the opening of a SDW gap. The slope change below T^* corresponds very well to the inflection point temperature of ρ. Thus, we conclude that T^* marks a temperature regime where the correlation length of the incipient SDW order drastically enhances.

At this point it is again instructive to compare these findings with the Hall data of LaFeAsO [22]. There, the Hall coefficient is in a similar way only weakly temperature dependent above the transition temperature. Below the closely connected T_N and T_S, the absolute value of the Hall coefficient increases by roughly one order of magnitude. Thus, except for the absolute values we have practically the same behavior in both Mn_3Si and LaFeAsO.

Early Hall effect measurements [56] on Cr seem to yield a similar anomaly at the SDW transition also in this compound, indicative of a significant change of the carrier density at the transition.

D. Thermal conductivity

The thermal conductivity plotted in Fig. 1(d) is nearly constant for temperatures above 150 K with a value of about $\kappa = 10\ \mathrm{W\,K^{-1}\,m^{-1}}$. Below this temperature κ rises to a maximum of $\kappa_{\max} = 114\ \mathrm{W\,K^{-1}\,m^{-1}}$ at 37 K and goes down rapidly for $T \to 0$ with a strong change in slope nearly at T_N. To understand the contributions to the thermal conductivity we estimated at first the electronic contribution by the Wiedemann–Franz-law:

$$\kappa = L\sigma T, \tag{1}$$

with $L = \frac{\pi^2}{3}(\frac{k_B}{e})^2 = 2.45 \times 10^{-8}\ \frac{\mathrm{W\Omega}}{\mathrm{K^2}}$, the theoretical result of the Drude–Sommerfeld theory. We compare κ/T with L/ρ in the inset of Fig. 1(d) in a log scale. This yields a sizable but still relatively small electronic contribution at high temperatures ($T \gtrsim 50$ K). At lower temperatures, L/ρ increases due to the drop of the resistivity but remains always one order of magnitude lower than κ. The inset also shows the difference $\kappa/T - L/\rho$, which demonstrates that electronic heat conduction plays a negligible role, especially at low temperatures.

The origin of the strong slope change at T_N remains unclear. On the one hand, it could arise from additional magnetic heat conduction of the magnetically ordered phase. On the other hand, the anomaly could also arise from a suppression of the low-temperature edge of the phonon peak near T_N, due to enhanced scattering of phonons off magnetic fluctuations. This is a common behavior for phononic heat conductivity of antiferromagnets with a significant magnon-phonon coupling, where the temperature regime of the peak coincides with the Néel temperature [57–59].

E. Seebeck effect

The Seebeck coefficient [see Fig. 1(e)] is negative over the whole measured temperature range, consistent with the negative sign of R_H. The Seebeck coefficient of Mn_3Si has a value of $S = -20\ \mu\mathrm{V/K}$ at 300 K and continuously falls to more negative values with decreasing temperature towards a pronounced anomaly with $S = -160\ \mu\mathrm{V/K}$ at 33 K approaching $S = 0\ \mu\mathrm{V/K}$ for $T \to 0$.

The transport equations yield the following expression for the thermopower [48]:

$$S = \frac{\pi^2}{3}\frac{k_B^2 T}{q}\left[\frac{\partial \ln \sigma\,(E)}{\partial E}\right]_{E=E_F}, \tag{2}$$

where q denotes the charge of the carriers, and $\sigma(E)$ stands for the electrical conductivity in dependence of the energy [48]. Since in Eq. (2) the Seebeck coefficient depends linearly on the temperature, it is worthwhile analyzing S/T [see inset of Fig. 1(e)]. The strong temperature dependence of this quantity apparently has to be ascribed to the quantity $\partial \ln \sigma(E)/\partial E$ which in the case of a momentum-independent mean-free path l_e may be broken down to [48]

$$\frac{\partial \ln \sigma\,(E)}{\partial E} = \frac{\partial \ln l_e}{\partial E} + \frac{\partial \ln A_{\mathrm{FS}}}{\partial E}. \tag{3}$$

Here, A_{FS} denotes the Fermi surface area.

Equation (3) suggests that the temperature dependence of S/T can be understood as stemming from separate contributions which are associated with the energy dependence of scattering processes and that of Fermi-surface topology changes. At $T \to \infty$ and at $T \to 0$ one expects the Fermi-surface topology to be robust and fluctuations (which presumably contribute to the first term) to be negligible. Thus S/T is expected to approach a constant value in both regimes. For the high-temperature limit this is clearly observed in the data, whereas the low-temperature limit is obviously not reached in the present data. While the pondering of these limits yields a clearcut physical picture, it is impossible to disentangle contributions of the two terms in Eq. (3) in the vicinity of the SDW transition where a strong temperature dependence is observed. It is interesting to describe the temperature dependence of S at intermediate temperatures by a single parameter only, i.e., the Fermi temperature T_F, which for $T \ll T_F$ contributes as [60]

$$S = \frac{\pi^2 k_B}{2q}\frac{T}{T_F}. \tag{4}$$

Thus, the changes for $T < 200$ K may be viewed as the consequence of Fermi temperature changes. Scattering processes and fluctuations freeze out at T_N and therefore S/T is expected to rapidly approach the low-temperature limit. This is reflected in the strong changes of S/T and the observed minimum. Note that the minimum is at a significantly larger temperature than T_N which means that the Seebeck coefficient responds already to a finite correlation length [33] at temperatures well above the ordered regime.

It is well known that, in addition to these purely electronic effects, the electron-phonon drag might play some role in the Seebeck effect. The drag effect becomes observable in a temperature range where the heat conductivity and thus the phononic mean-free path is high [48]. Interestingly, the phonon heat conductivity (see Fig. 1) peaks at the same temperature as the Seebeck coefficient. From the Seebeck effect data alone it remains unclear whether this is just coincidental, or if this indicates a significant importance of the electron-phonon drag. Further below we argue based on our Nernst effect data that

a phonon drag is unimportant for explaining the discussed behavior of the Seebeck coefficient.

The comparison with Seebeck coefficient data [22,53,61] for LaFeAsO and Cr shows that the observed characteristics, namely a fluctuation regime at $T > T_N$ and a sharp change of S at T_N, are apparently generic features at SDW transitions. Interestingly, the contributions in the fluctuation regime and at $T \lesssim T_N$ have the same sign in both LaFeAsO and Cr, whereas their sign is opposite in Mn_3Si. We attribute these differences to details of the band structure.

F. Nernst effect

For measuring the Nernst effect a temperature gradient is applied along the x direction of the sample in the presence of a magnetic field B along the z axis. The Nernst signal N is a voltage drop as the signature of an electric field E_y along the y direction of the sample [26,60]. In nonsuperconducting metals the Nernst signal is expected to be linear in magnetic field. Thus one defines the Nernst coefficient as

$$\nu_N = \frac{N}{B} = \frac{E_y}{|-\partial_x T|B}. \tag{5}$$

We are using the new sign convention after which a superconducting vortex would give a positive contribution to ν_N [60]. In compounds in which the phononic heat conductivity is far higher than the electronic contribution to the heat conductivity, as is the case in Mn_3Si at low temperature, one can write for the Nernst coefficient [62]

$$\nu_N = \left[\frac{\alpha_{xy}}{\sigma_{xx}} - S_{xx}\tan\theta\right]\frac{1}{B}, \tag{6}$$

where α_{xy} denotes the nondiagonal Peltier coefficient and $\tan\theta = \frac{\sigma_{xy}}{\sigma_{xx}}$ is the Hall angle. In a simple one-band metal the two terms on the right-hand side are expected to cancel each other out exactly, which is often called the Sondheimer cancellation. It can be shown that, in multiband metals and in superconductors in the mixed state, Sondheimer's rule is violated [26,60]. The Nernst coefficient may therefore be considered as a measure to what extent a metal deviates from a simple one-band metal.

An alternative expression for the Nernst coefficient is given by [60,63]

$$\nu_N = -\frac{\pi^2}{3}\frac{k_B^2 T}{eB}\left[\frac{\partial\tan\theta}{\partial E}\right]_{E=E_F}. \tag{7}$$

In this formulation Sondheimer's cancellation corresponds to the exact vanishing of the energy dependence of the Hall angle [60]. Since the prefactor in Eq. (7) is linear in temperature, and the Hall angle depends on both the carrier scattering rate and the carriers effective mass, one may qualitatively analyze the temperature dependence of the Nernst coefficient in a similar way as that of the Seebeck coefficient, as will be discussed further below.

In the case of Mn_3Si the Nernst coefficient at room temperature is very small, ~ 1 nV K^{-1} T^{-1}, and decreases roughly linearly to zero at about 150 K where $\nu_N(T)$ changes its slope to a somewhat larger value. At 44 K a kink appears and the Nernst coefficient decreases even stronger with decreasing temperature towards a minimum value of -8.2 nV K^{-1} T^{-1} at $\sim$20 K. This is almost exactly the temperature of the inflection point in the resistivity and that of the maximum of the specific-heat anomaly, i.e., T_N. At lower temperatures, and thus deep in the magnetic regime, the Nernst coefficient increases strongly towards $\nu_N = 3.16 \times 10^{-2}$ μV K^{-1} T^{-1} at the lowest measured temperature of 7 K.

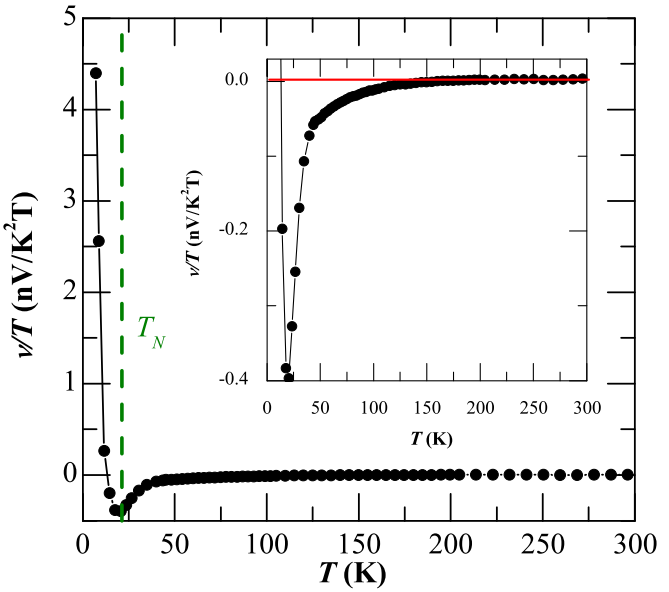

FIG. 3. (Color online) Nernst coefficient ν/T of Mn_3Si(dots). Inset: Nernst coefficient plotted with a constant line at $\nu = 0$.

ν_N/T, which is plotted in Fig. 3, is very small and temperature independent at $T \geqslant 150$ K, which shows that Mn_3Si in this temperature regime behaves as an ordinary metal in line with the linear resistivity at $T > 200$ K. The strong temperature dependence at lower temperature according to Eq. (7) stems from the energy dependence of the Hall angle and implies strong changes in the scattering time and the effective mass. It is clear that both quantities experience strong variations in the fluctuation regime. Therefore we cannot distinguish between these two contributions in the Nernst coefficient. In a similar way as with the Seebeck coefficient we can understand the temperature dependence of the Nernst coefficient in terms of a fluctuation regime in the range $T_N < T < 150$ K where the Fermi temperature changes and a regime with a qualitatively different behavior at lower temperatures.

We point out that the temperature dependence of the Nernst and Seebeck coefficients is qualitatively very similar. However, we note that, despite the similarities at the high- and low-temperature regimes, in the intermediate-temperature regime $T_N < T < 50$ K the temperature dependencies of the two effects are remarkably different. This concerns mostly the temperature of the minimum in the vicinity of T_N. These similarities as well as the differences appear plausible in view of a simplified expression [60]

$$\frac{\nu}{T} \sim \frac{1}{T_F}\mu. \tag{8}$$

Both quantities depend in a similar way on T_F but the Nernst effect is amplified by μ (see Fig. 4). This explains qualitatively

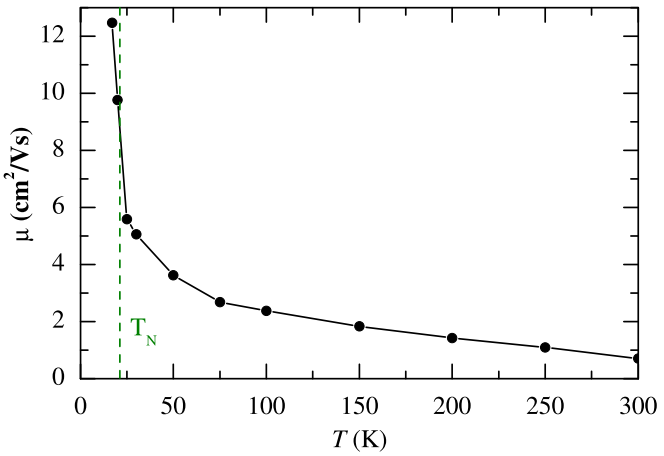

FIG. 4. (Color online) Calculated one-band mobility μ of Mn_3Si(dots).

the shift of the minimum in temperature comparing the Seebeck and the Nernst coefficient. This illustrates that the measurement of the Nernst effect is a remarkable and powerful complementary method to more conventional transport coefficients which underpins that this quantity is extremely sensitive to fluctuations of the Fermi-surface topology. On a further note, we point out that phonons are not influenced by the magnetic field which implies that due to the similarity of the temperature dependence of ν and S the electron-phonon drag plays only a minor role in the Seebeck coefficient.

We again compare these findings with results for LaFeAsO [22], where it is observed that the Nernst coefficient is nearly constant and zero at $T \gg T_N$. Upon approaching the SDW transition from above, corresponding fluctuations have also been reported to lead to an enhanced Nernst response, which increases even further below the SDW transition. Note that in LaFeAsO the fluctuation-enhanced and the SDW-enhanced Nernst coefficient are of the same sign, whereas the respective signs are opposite in Mn_3Si.

IV. CONCLUSION

In conclusion, we investigated a comprehensive set of transport coefficients on a single crystalline sample of the itinerant antiferromagnet Mn_3Si. All transport coefficients except the thermal conductivity are sensitive to the SDW transition in this material and exhibit strong anomalies around the ordering temperature $T_N \sim 21.3$ K. These anomalies qualitatively arise from both strongly-temperature-dependent changes of the relaxation time and of the Fermi-surface topology in relation to the SDW transition. Such transport investigations are therefore an important and powerful tool for disentangling the nontrivial nature of the magnetism of itinerant electron systems. This is further demonstrated by the apparent generic nature of many of the observed characteristics related to the phase transition, which are deduced from comparison with similar studies on other prototype SDW compounds. We point out that the rarely studied Nernst effect apparently provides a rather rich spectrum of information which underpins the potential of this quantity for experiments in solid state physics.

An interesting finding which is evident in Mn_3Si from the resistivity, Seebeck-coefficient, and Nernst-coefficient data is a large fluctuation regime which extends up to about 200 K. Fluctuations which evolve already at temperatures almost one order of magnitude higher than the actual ordering temperature appear rather unusual for a three-dimensional metal. One might speculate that this large fluctuation regime is the signature of competing orders in the compound. This notion is nourished by the theoretical finding of a second nesting vector in the electronic structure which is calculated to cause an even stronger instability than that related to the actual observed order [38,39].

ACKNOWLEDGMENTS

This work was supported by the Deutsche Forschungsgemeinschaft through SPP 1538, Grant HE 3439/9, and through GRK 1621. S. Wurmehl acknowledges funding by DFG in project WU 595/3-1 (Emmy–Noether program).

[1] J. M. Tranquada, B. J. Sternlieb, J. D. Axe, Y. Nakamura, and S. Uchida, Nature (London) **375**, 561 (1995).
[2] J. M. Tranquada, H. Woo, T. G. Perring, H. Goka, G. D. Gu, G. Xu, M. Fujita, and K. Yamada, Nature (London) **429**, 534 (2004).
[3] J. Fink, V. Soltwisch, J. Geck, E. Schierle, E. Weschke, and B. Büchner, Phys. Rev. B **83**, 092503 (2011).
[4] F. Laliberté, J. Chang, N. Doiron-Leyraud, E. Hassinger, R. Daou, M. Rondeau, B. Ramshaw, R. Liang, D. Bonn, W. Hardy *et al.*, Nat. Commun. **2**, 432 (2012).
[5] J. Chang, E. Blackburn, A. T. Holmes, N. B. Christensen, J. Larsen, J. Mesot, R. Liang, D. A. Bonn, W. N. Hardy, A. Watenphul *et al.*, Nat. Phys. **8**, 871 (2012).
[6] J. C. S. Davis and D.-H. Lee, Proc. Natl. Acad. Sci. USA **110**, 17623 (2013).
[7] E. Fradkin and S. A. Kivelson, Nat. Phys. **8**, 864 (2012).
[8] Y. Kamihara, T. Watanabe, M. Hirano, and H. Hosono, J. Am. Chem. Soc. **130**, 3296 (2008).
[9] H.-H. Klauss, H. Luetkens, R. Klingeler, C. Hess, F. J. Litterst, M. Kraken, M. M. Korshunov, I. Eremin, S.-L. Drechsler, R. Khasanov *et al.*, Phys. Rev. Lett. **101**, 077005 (2008).
[10] H. Luetkens, H.-H. Klauss, M. Kraken, F. J. Litterst, T. Dellmann, R. Klingeler, C. Hess, R. Khasanov, A. Amato, C. Baines *et al.*, Nat. Mater. **8**, 305 (2009).
[11] R. M. Fernandes and J. Schmalian, Phys. Rev. B **82**, 014521 (2010).
[12] R. M. Fernandes, D. K. Pratt, W. Tian, J. Zarestky, A. Kreyssig, S. Nandi, M. G. Kim, A. Thaler, N. Ni, P. C. Canfield *et al.*, Phys. Rev. B **81**, 140501 (2010).
[13] P. Dai, J. Hu, and E. Dagotto, Nat. Phys. **8**, 709 (2012).
[14] K. W. Kim, A. Pashkin, H. Schäfer, M. Beyer, M. Porer, T. Wolf, C. Bernhard, J. Demsar, R. Huber, and A. Leitenstorfer, Nat. Mater. **11**, 497 (2012).
[15] Z. P. Yin, K. Haule, and G. Kotliar, Nat. Phys. **7**, 294 (2011).
[16] R. Bel, K. Behnia, and H. Berger, Phys. Rev. Lett. **91**, 066602 (2003).

[17] R. Bel, H. Jin, K. Behnia, J. Flouquet, and P. Lejay, Phys. Rev. B **70**, 220501 (2004).

[18] J. Chang, R. Daou, C. Proust, D. LeBoeuf, N. Doiron-Leyraud, F. Laliberté, B. Pingault, B. J. Ramshaw, R. Liang, D. A. Bonn *et al.*, Phys. Rev. Lett. **104**, 057005 (2010).

[19] O. Cyr-Choiniére, R. Daou, F. Laliberte, D. LeBoeuf, N. Doiron-Leyraud, J. Chang, J. Q. Yan, J. G. Cheng, J. S. Zhou, J. B. Goodenough *et al.*, Nature (London) **458**, 743 (2009).

[20] R. Daou, J. Chang, D. LeBoeuf, O. Cyr-Choiniére, F. Laliberté, F. N. Doiron-Leyraud, B. J. Ramshaw, R. Liang, D. A. Bonn, W. N. Hardy *et al.*, Nature (London) **463**, 519 (2010).

[21] C. Hess, E. Ahmed, U. Ammerahl, A. Revcolevschi, and B. Büchner, Eur. Phys. J. Spec. Top. **188**, 103 (2010).

[22] A. Kondrat, G. Behr, B. Büchner, and C. Hess, Phys. Rev. B **83**, 092507 (2011).

[23] A. Hackl, M. Vojta, and S. Sachdev, Phys. Rev. B **81**, 045102 (2010).

[24] A. Pourret, H. Aubin, J. Lesueur, C. A. Marrache-Kikuchi, L. Berg, L. Dumoulin, and K. Behnia, Nat. Phys. **2**, 683 (2006).

[25] Z. A. Xu, N. Ong, Y. Wang, T. Kakeshita, and S. Uchida, Nature (London) **406**, 486 (2000).

[26] Y. Wang, L. Li, and N. P. Ong, Phys. Rev. B **73**, 024510 (2006).

[27] S. Tomiyoshi and H. Watanabe, J. Phys. Soc. Jpn. **39**, 295 (1975).

[28] S. Tomiyoshi, S. Funahashi, and Y. Yamaguchi, Physica B + C (Amsterdam) **120**, 143 (1983).

[29] S. Tomiyoshi, E. R. Cowley, and H. Onodera, Phys. Rev. B **73**, 024416 (2006).

[30] S. Tomiyoshi, Y. Yamaguchi, M. Ohashi, E. R. Cowley, and G. Shirane, Phys. Rev. B **36**, 2181 (1987).

[31] C. Pfleiderer, J. Bœuf, and H. v. Löhneysen, Phys. Rev. B **65**, 172404 (2002).

[32] B. Aronson, Acta Chem. Scand. **14**, 1414 (1960).

[33] Y. Yamaguchi, T. Thurston, H. Miki, and S. Tomiyoshi, Phys. B (Amsterdam, Neth.) **213**, 363 (1995).

[34] S. Tomiyoshi, H. Ohsumi, H. Kobayashi, and A. Yamamoto, J. Phys. Soc. Jpn. **83**, 044715 (2014).

[35] M. Hortamani, L. Sandratskii, P. Zahn, and I. Mertig, J. Appl. Phys. **105**, 07E506 (2009).

[36] S. Wurmehl, H. C. Kandpal, G. H. Fecher, and C. Felser, J. Phys.: Condens. Matter **18**, 6171 (2006).

[37] J. Kübler, A. R. Williams, and C. B. Sommers, Phys. Rev. B **28**, 1745 (1983).

[38] P. Mohn and E. Supanetz, Philos. Mag. B **78**, 629 (1998).

[39] A. V. Vlasov, E. T. Kulatov, and A. A. Povzner, Sov. Phys. Lebedev Inst. Rep. **12**, 5 (1990).

[40] C. Pfleiderer, Phys. B (Amsterdam, Neth.) **329** (Part 2), 1085 (2003).

[41] H. van Leuken and R. A. de Groot, Phys. Rev. Lett. **74**, 1171 (1995).

[42] T. Jeong, Phys. B (Amsterdam, Neth.) **407**, 888 (2012).

[43] M. Doerr, J. Bœuf, C. Pfleiderer, M. Rotter, N. Kozlova, D. Eckert, P. Kerschl, K.-H. Müller, and M. Loewenhaupt, Phys. B (Amsterdam, Neth.) **346**, 137 (2004).

[44] R. Hermann, H. Wendrock, S. Rodan, U. Rler, C. Blum, S. Wurmehl, and B. Büchner, J. Cryst. Growth **363**, 1 (2013).

[45] R. Hermann, G. Behr, G. Gerbeth, J. Priede, H.-J. Uhlemann, F. Fischer, and L. Schultz, J. Cryst. Growth **275**, e1533 (2005).

[46] C. Hess, B. Büchner, U. Ammerahl, and A. Revcolevschi, Phys. Rev. B **68**, 184517 (2003).

[47] C. Hess, A. Kondrat, A. Narduzzo, J. E. Hamann-Borrero, R. Klingeler, J. Werner, G. Behr, and B. Büchner, Europhys. Lett. **87**, 17005 (2009).

[48] J. M. Ziman, *Electrons and Phonons* (Clarendon Press, Oxford, 2003).

[49] D. Bombor, C. G. F. Blum, O. Volkonskiy, S. Rodan, S. Wurmehl, C. Hess, and B. Büchner, Phys. Rev. Lett. **110**, 066601 (2013).

[50] K. Ueda, J. Phys. Soc. Jpn. **43**, 1497 (1977).

[51] S. I. Masharov, Phys. Status Solidi B **21**, 747 (1967).

[52] M. A. McGuire, A. D. Christianson, A. S. Sefat, B. C. Sales, M. D. Lumsden, R. Jin, E. A. Payzant, D. Mandrus, Y. Luan, V. Keppens *et al.*, Phys. Rev. B **78**, 094517 (2008).

[53] J. P. Moore, R. K. Williams, and R. S. Graves, J. Appl. Phys. **48**, 610 (1977).

[54] E. Fawcett, Rev. Mod. Phys. **60**, 209 (1988).

[55] S. Fujii, S. Ishida, and S. Asano, J. Phys. Soc. Jpn. **64**, 185 (1995).

[56] G. D. Vries and G. Rathenau, J. Phys. Chem. Solids **2**, 339 (1957).

[57] G. A. Slack and R. Newman, Phys. Rev. Lett. **1**, 359 (1958).

[58] G. Laurence and D. Petitgrand, Phys. Rev. B **8**, 2130 (1973).

[59] G. A. Slack, Phys. Rev. **122**, 1451 (1961).

[60] K. Behnia, J. Phys.: Condens. Matter **21**, 113101 (2009).

[61] A. Kondrat, J. E. Hamann-Borrero, N. Leps, M. Kosmala, O. Schumann, A. Köhler, J. Werner, G. Behr, M. Braden, R. Klingeler *et al.*, Eur. Phys. J. B **70**, 461 (2009).

[62] Y. Wang, Z. A. Xu, T. Kakeshita, S. Uchida, S. Ono, Y. Ando, and N. P. Ong, Phys. Rev. B **64**, 224519 (2001).

[63] V. Oganesyan and I. Ussishkin, Phys. Rev. B **70**, 054503 (2004).